Chapter 8

In Vivo Tumor Angiogenesis Imaging Using Peptide-Based Near-Infrared Fluorescent Probes

Rui Huang, Peter S. Conti, and Kai Chen

Abstract

Near-infrared fluorescence (NIRF) imaging is an emerging imaging technique for studying diseases at the molecular level. Optical imaging with a near-infrared emitting fluorophore for targeting tumor angiogenesis offers a noninvasive method for early tumor detection and efficient monitoring of tumor response to anti-angiogenesis therapy. CD13 receptor, a zinc-dependent membrane-bound ectopeptidase, plays important roles in regulating tumor angiogenesis and the growth of new blood vessels. In this chapter, we use CD13 receptor as an example to demonstrate how to construct CD13-specific NGR-containing peptides via bioorthogonal click chemistry for visualizing and quantifying the CD13 receptor expression in vivo by means of NIRF optical imaging.

Key words Tumor angiogenesis, Near-infrared fluorescence imaging, Peptide-based probes, Molecular imaging, Cancer

1 Introduction

Near-infrared fluorescence (NIRF) imaging is an excellent noninvasive technique for studying diseases at the molecular level in living subjects [1–4]. As an excellent complement to nuclear imaging techniques, such as positron emission tomography (PET) and single-photon emission computed tomography (SPECT), NIRF imaging does not employ ionizing radiation or radioactive materials, rendering it cost-effective, robust, sensitive, and straightforward over other imaging modalities [3, 5, 6]. Although absorption and scattering from biological tissues may limit penetration of light through the body, photon penetration into and out of tissue can be more efficient in the near-infrared window (650–900 nm) with minimal intra-tissue scattering. Recent research advances have demonstrated that NIRF imaging is playing a valuable role in better understanding of biology, early diagnosis of diseases, and effective assessment of treatment [7–9].

Mingfeng Bai (ed.), *In Vivo Fluorescence Imaging: Methods and Protocols*, Methods in Molecular Biology, vol. 1444,
DOI 10.1007/978-1-4939-3721-9_8,

Angiogenesis, the formation of new blood vessels from pre-existing vasculature, is a fundamental process occurring during tumor progression [10–13]. A sizable body of evidence suggests that the formation of tumor angiogenesis is a complex multi-step process that follows a characteristic sequence of events mediated and controlled by growth factors, cellular receptors, and adhesion molecules [14–16]. Therefore, biomarkers exclusively expressed in tumor angiogenesis can be recognized as potential targets for cancer diagnosis and therapy. Numerous studies have proved that CD13 receptor is an important regulator of endothelial morphogenesis during tumor angiogenesis [17]. CD13 receptor, also known as aminopeptidase N (APN), is a zinc-dependent membrane-bound ectopeptidase that degrades preferentially proteins and peptides with an *N*-terminal neutral amino acid [18]. Research results suggest that overexpression of CD13 is associated with the progression of many tumors, such as prostate, colon, and pancreatic cancer [19–21]. Through in vivo screening of a phage-displayed peptide library, a tumor vasculature homing phage carrying sequence CNGRCVSGCAGRC was selected by using human breast carcinoma xenografts [22]. Later, the molecular basis behind NGR tumor-homing properties was revealed, and NGR-containing peptide was identified as a specific ligand for CD13 receptor [23]. Consequently, a number of NGR-containing derivatives have been developed for both CD13-targeted tumor imaging and therapy [6, 24–30].

Click chemistry offers chemists a platform for modular and high-yielding synthetic transformations for constructing highly diverse molecules [31]. The Huisgen 1,3-dipolar cycloaddition reaction, which fuses an azide and an alkyne together, and provides access to a variety of five-membered heterocycles, has become of great use in the development of new molecular probes [32]. Based on our previous experience [33], a catalyst-free click chemistry system using the ligation of dibenzocyclooctyne and azide was chosen to prepare peptide-based near-infrared fluorescent probes (Fig. 1) [34, 35]. To this end, the dimeric NGR peptide (NGR2) was conjugated with an azide-terminated Cy5.5 fluorophore (Cy5.5-N_3) to rapidly afford Cy5.5-NGR2 in a quantitative yield. The Cy5.5-NGR2 peptide provided highly sensitive and target-specific imaging of CD13 receptor expression in tumors. The excellent tumor-to-normal tissue ratio and fast

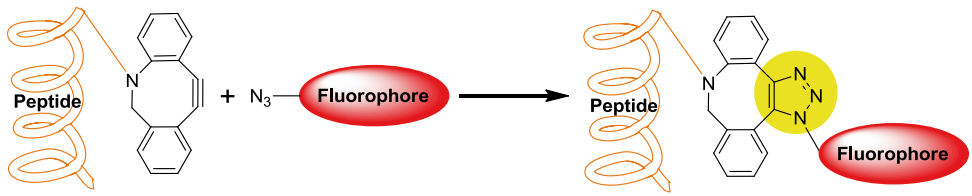

Fig. 1 Schematic representation of the construction of peptide-based near-infrared fluorescent probe via bioorthogonal click chemistry for in vivo tumor angiogenesis imaging

tumor targeting ability of Cy5.5-NGR2 have proved it a promising molecular probe, not only allowing the NIRF imaging of CD13 overexpressed tumor angiogenesis, but also having the potential to facilitate noninvasive monitoring of CD13-targeted anti-angiogenesis therapy.

2 Materials

Prepare all solutions using ultrapure water (prepared by purifying deionized water) and analytical grade reagents. Prepare and store all reagents at room temperature (unless indicated otherwise). Diligently follow all waste disposal regulations when disposing waste materials.

1. Monomeric NGR peptide [GGGCNGRC; disulfide Cys:Cys = 4 – 8] (C S Bio, Inc., Menlo Park, CA, USA).
2. Dimeric NGR peptide (NGR2) is prepared using the reported procedure [30].
3. Cy5.5 azide (Cy5.5-N_3) (Lumiprobe, Hallandale Beach, FL, USA).
4. DBCO-PEG_4-NHS ester (Click Chemistry Tools, Inc., Scottsdale, AZ, USA).
5. Sodium borate buffer (pH 8.5).
6. Phosphate-buffered saline (PBS).
7. 0.1% TFA in water (Solution A, which has been rigorously degassed for high-performance liquid chromatography [HPLC] use).
8. 0.1% TFA in acetonitrile (Solution B, which has been rigorously degassed for HPLC use).
9. Luna C18 reversed phase column (5 μm, 250 × 4.6 mm) (Phenomenex, Torrance, CA, USA).
10. Chamber slides (VWR Corporate, Radnor, PA, USA).
11. Dulbecco's modified Eagle's medium (DMEM) (USC Cell Culture Core, Los Angeles, CA, USA).
12. HT-1080 human fibrosarcoma cell line (ATCC, Manassas, VA, USA).
13. MCF-7 human breast cancer cell line (ATCC, Manassas, VA, USA).
14. Fetal bovine serum (FBS).
15. Paraformaldehyde (PFA).
16. Matrigel (BD Biosciences, San Jose, CA, USA).
17. Female athymic nude mice (Harlan Laboratories, Livermore, CA, USA).

3 Methods

3.1 Preparation of DBCO-Conjugated NGR2 Peptide

1. Dissolve the dimeric NGR peptide (NGR2) (2.6 μmol) in 200 μL of sodium borate buffer (pH = 8.5).
2. Add DBCO-PEG_4-NHS ester (3.1 μmol) dissolved in 20 μL of DMSO.
3. Adjust the mixture to pH 8.5 (*see* **Note 1**).
4. Sonicate at room temperature for 1 h.
5. Purify the crude peptide by HPLC (*see* **Note 2**).
6. Collect the peak containing the desired product.
7. Lyophilize to afford a fluffy white powder (*see* **Note 3**).

3.2 Preparation of Cy5.5-NGR2 Peptide

1. Dissolve the DBCO-conjugated NGR2 peptide (0.48 μmol) in 100 μL of PBS.
2. Add Cy5.5-N_3 (0.53 μmol) in 10 μL of DMSO and 100 μL of acetonitrile (*see* **Note 4**).
3. Shake the mixture in the dark at room temperature for 15 min.
4. Purify the crude peptide by HPLC (*see* **Note 5**).
5. Collect the peak containing the desired product.
6. Lyophilize to afford Cy5.5-NGR2 peptide (*see* **Note 6**).

The chemical structure of Cy5.5-NGR2 peptide is illustrated in Fig. 2.

3.3 Absorption and Emission Spectra of Cy5.5-NGR2 Peptide

1. The absorption spectrum of Cy5.5-NGR2 peptide is recorded on a Cary 14 UV-Vis spectrometer (Bogart, GA, USA). The spectrum is scanned from 550 to 800 nm with an increment of 1 nm.
2. The fluorescence emission of Cy5.5-NGR2 peptide is measured using a Shimadzu RF-5301PC spectrofluorophotometer (Columbia, MD, USA), and the spectrum is scanned from 550 to 800 nm with an increment of 1 nm. The wavelength of excitation light is set at 650 nm.

The absorption and emission fluorescence spectra of Cy5.5-NGR2 peptide in deionized water are illustrated in Fig. 3.

3.4 Binding Specificity of Cy5.5-NGR2 to CD13 Receptor

1. HT-1080 and MCF-7 cells are grown in DMEM supplemented with 10% FBS at 37 °C in humidified atmosphere containing 5% CO_2.
2. HT-1080 and MCF-7 cells are grown in chamber slides with a density of 2×10^4/well for 24 h.
3. Wash cells with serum-free DMEM medium for 3 min, fix cells in each well with 2% PFA for 10 min, and then wash cells with serum-free DMEM medium (three times, 3 min/wash).

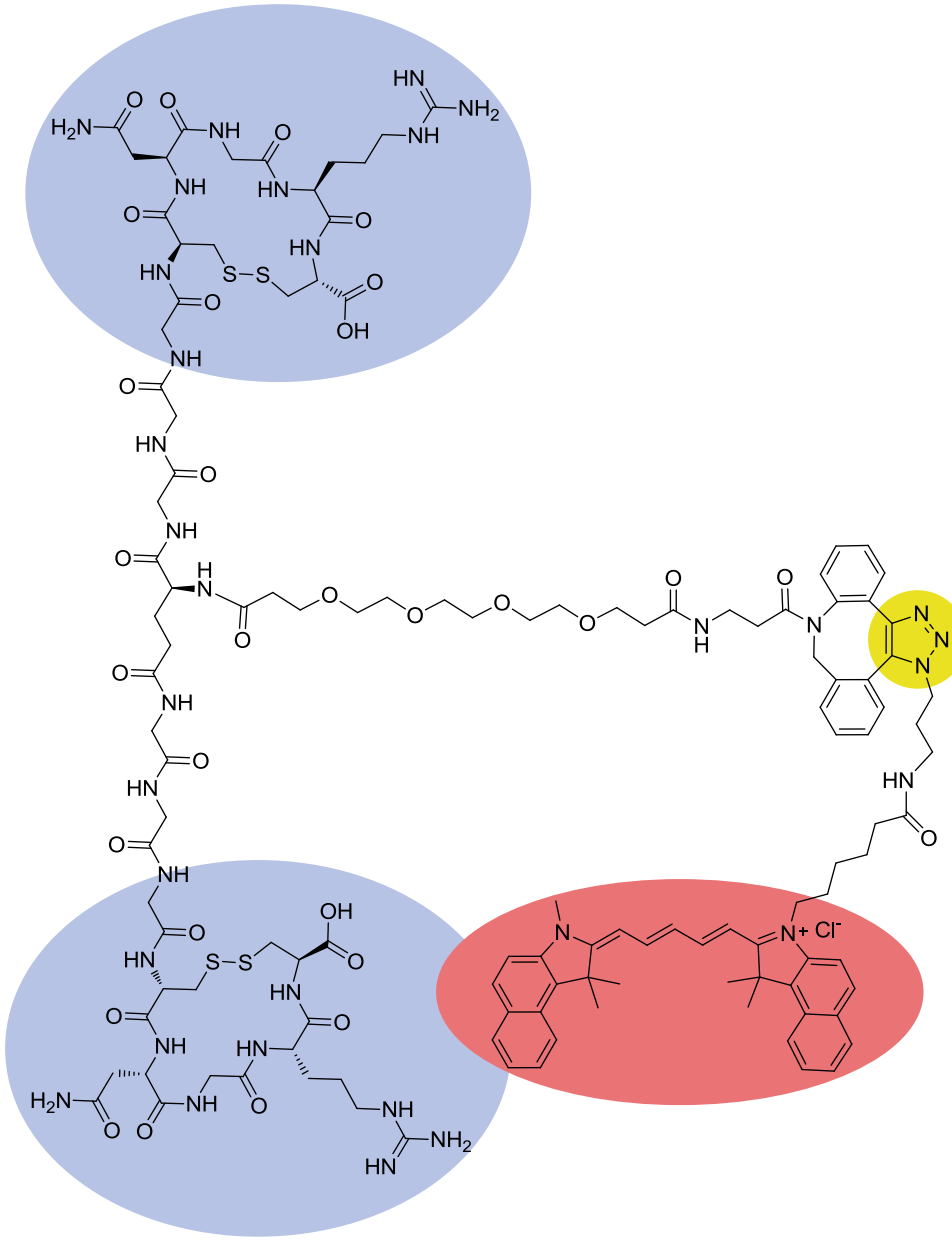

Fig. 2 Schematic structure of Cy5.5-NGR2 peptide. *Blue*: NGR peptide; *red*: Cy5.5 dye. Reproduced from Ref. 6 with permission from Springer

4. Add 20 nM of Cy5.5-NGR2 peptide in 200 μL of serum-free DMEM medium to the HT-1080 or MCF-7 cells.
5. Incubate at 37 °C in the dark for 15 min.
6. Wash cells with PBS (three times, 5 min/wash).
7. For the blocking group, the HT-1080 cells are co-incubated with 20 nM of Cy5.5-NGR2 peptide and 50 μM of non-labeled monomeric NGR peptide (*see* **Note** 7).

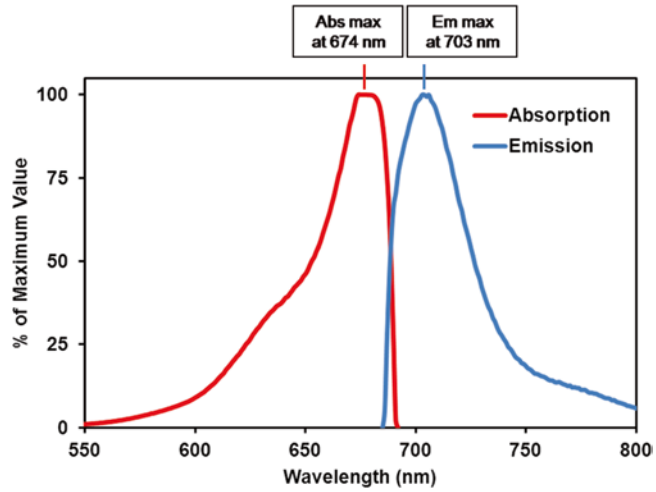

Fig. 3 Absorption and emission fluorescence spectra of Cy5.5-NGR2 peptide. Reproduced from Ref. 6 with permission from Springer

8. Mount the chamber slides with a 4′,6-diamidino-2-phenylindole (DAPI)-containing mounting medium.
9. Place the slides under a Zeiss LSM 510 confocal laser scanning microscope (Carl Zeiss Microscopy, LLC, Thornwood, NY, USA) with a Cy5 filer and record the images at 633 nm excitation wavelength.

It is critical that the CD13-binding specificity is maintained after chemical modification of NGR peptides (*see* **Note 8**). A representative result is shown in Fig. 4.

3.5 In Vivo NIRF Optical Imaging

1. Generate the tumor xenografts by subcutaneous injection of five million HT-1080 cells suspended in 50 μL of cell culture media and 50 μL of BD Matrigel into the right shoulder of female athymic nude mice (Harlan Laboratories, Livermore, CA, USA) (*see* **Note 9**). The mice are subjected to in vivo NIRF imaging studies when the tumor volume reaches 200–300 mm^3 (about 2 weeks after inoculation). Monitor the tumor volume every other day using a caliper following the formula $V = (witdth)^2 \times length / 2$.
2. Set up the IVIS Imaging System 200 Series (PerkinElmer Inc., Alameda, CA, USA). A Cy5.5 filter set is used to acquire the fluorescent signals.
3. Obtain the fluorescent signals by scanning a tumor-bearing mouse before the injection of Cy5.5-NGR2.
4. Inject 1.5 nmol of Cy5.5-NGR2 into a tumor-bearing mouse via the tail vein while the mouse is under isoflurane anesthesia.
5. For the blocking experiment, inject 1.5 nmol of Cy5.5-NGR2 with a non-labeled monomeric NGR peptide (20 mg/kg) into a tumor-bearing mouse via the tail vein.

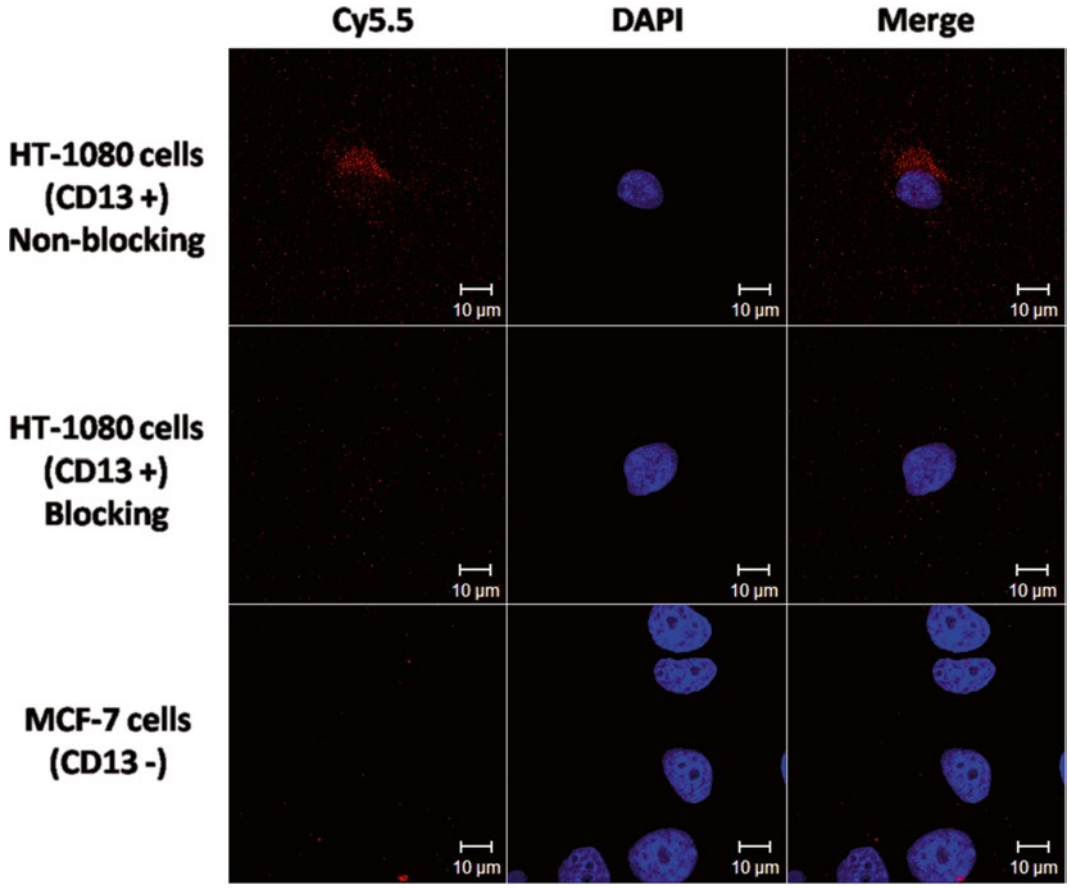

Fig. 4 Confocal microscopy results of Cy5.5-NGR2 with HT-1080 cells (CD13 positive) and MCF-7 cells (CD13 negative) (magnification: 100×). The blocking study is achieved by adding unlabeled monomeric NGR peptide. *Top*: Incubation of Cy5.5-NGR2 (20 nM) with CD13-positive HT-1080 cells; *middle*: incubation of Cy5.5-NGR2 (20 nM) with CD13-positive HT-1080 cells blocked by a non-labeled monomeric NGR peptide (50 μM); *bottom*: incubation of Cy5.5-NGR2 (20 nM) with CD13-negative MCF-7 cells. Reproduced from Ref. 6 with permission from Springer

6. Scan the animal at 0.5, 1, 2, 3, and 4 h (*see* **Note 10**). The identical illumination settings (lamp voltage, filters, f/stop, field of views, binning) are used to acquire all images. All NIRF images are acquired using 1-s exposure time (f/stop = 4). Fluorescence emission images are normalized and reported as photons per second per centimeter squared per steradian (p/s/cm^2/sr) (*see* **Note 11**).

Representative NIRF images are shown in Fig. 5 after HT-1080 tumor-bearing mice are injected with 1.5 nmol of Cy5.5-NGR2. To determine tumor contrast, mean fluorescence intensities of the tumor area at the right shoulder of the animal and of the normal tissue at the surrounding tissue are calculated using the region-of-interest (ROI)

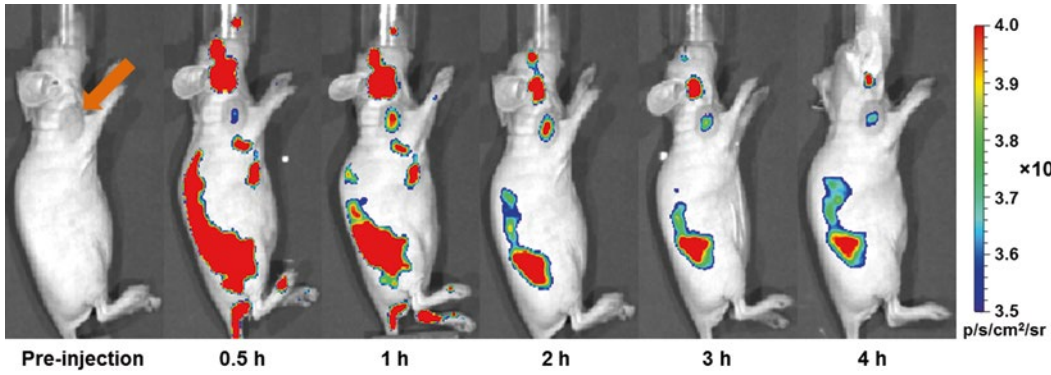

Fig. 5 Time-course fluorescence imaging of subcutaneous HT-1080 tumor-bearing nude mice after intravenous injection of 1.5 nmol of Cy5.5-NGR2. The tumors are clearly visualized as indicated by an *arrow* from 0.5 to 4 h pi. The fluorescence intensity is recorded as per second per centimeter squared per steradian (p/s/cm^2/sr). Reproduced from Ref. 6 with permission from Springer

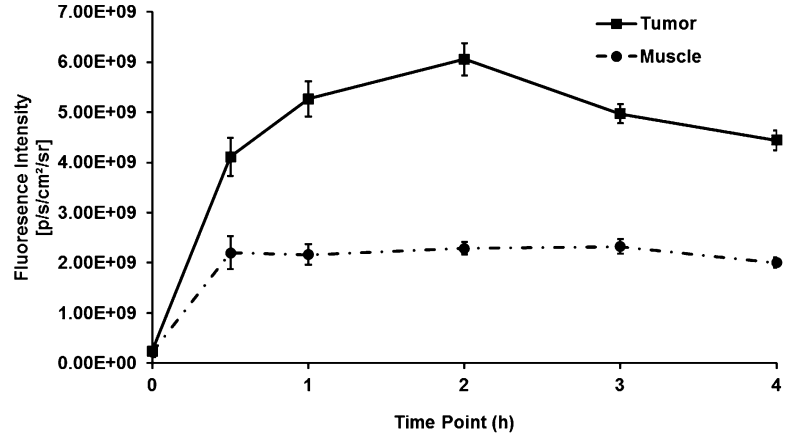

Fig. 6 Quantification and kinetics of in vivo targeting character of Cy5.5-NGR2 in the HT-1080 tumor vs. muscle. The Cy5.5-NGR2 uptake in HT-1080 tumor at various time points is significantly higher than that in muscle. *Error bar* is calculated as the standard deviation ($n=3$). Reproduced from Ref. 6 with permission from Springer

function of the IVIS Living Image 4.4 software (PerkinElmer Inc., Alameda, CA, USA). The fluorescence signal resulting from Cy5.5-NGR2 is clearly visible and the tumor fluorescence intensity reaches maximum at 2 h post-injection (Fig. 6). The NIRF images of HT-1080 tumor-bearing mice at 2 h pi from the non-blocking and blocking group are presented in Fig. 7. Tumor contrast as quantified by the ROI analysis of images shows that the tumor-to-muscle value at 2 h pi is reduced from 2.65 ± 0.13 to 1.05 ± 0.06 ($P<0.05$) by blocking CD13 receptor with a non-labeled NGR peptide (Fig. 8) (*see* **Note 12**).

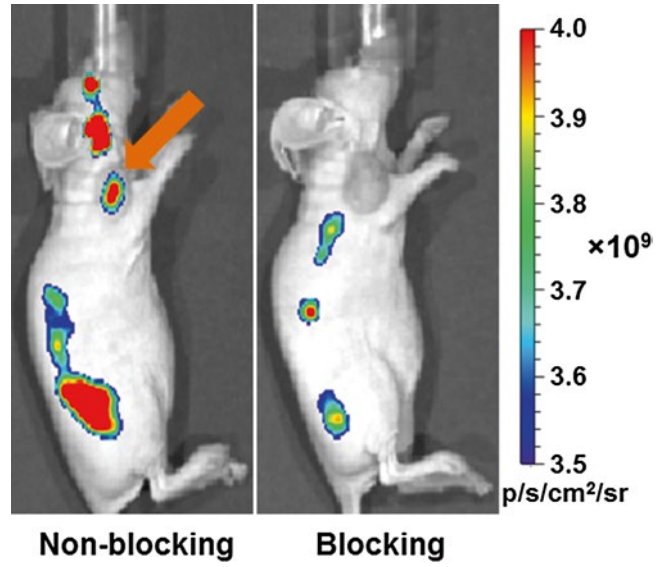

Fig. 7 Representative optical imaging (at 2 h pi) of mice bearing HT-1080 tumor on the right shoulder demonstrating blocking of Cy5.5-NGR2 (1.5 nmol) uptake by co-injection with a non-labeled monomeric NGR peptide (20 mg/kg). Reproduced from Ref. 6 with permission from Springer

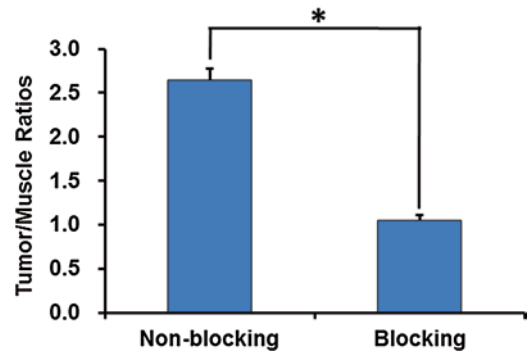

Fig. 8 Fluorescence intensity ratio of tumor to muscle based on the ROI analysis of Cy5.5-NGR2 uptake at 2 h pi in HT-1080 tumors without (non-blocking) or with (blocking) co-injection of a non-labeled monomeric NGR peptide (20 mg/kg). *Error bar* is calculated as the standard deviation ($n = 3$). Reproduced from Ref. 6 with permission from Springer

4 Notes

1. It is critical to adjust the pH value of mixture to 8.5 for amide bond formation between a succinimide ester and an amino group.
2. The flow rate is 1 mL/min with the mobile phase starting from 100% solvent A (0.1% TFA in water) to 40% solvent A and 60% solvent B (0.1% TFA in acetonitrile) at 22.5 min.

3. A typical yield is between 70 and 80%.
4. The selection of NIR optical dyes for in vivo cancer imaging is referred to the literature [36].
5. The flow rate is 1 mL/min with the mobile phase starting from 100% solvent A (0.1% TFA in water) to 5% solvent A and 95% solvent B (0.1% TFA in acetonitrile) at 30 min.
6. A typical yield is between 90 and 95%. The fluorescent peptide is stored as a dry powder in the dark at −20 °C until use.
7. To achieve the blocking experiment, various concentrations of non-labeled NGR peptide are tested. However, if the concentration of blocking NGR peptide is too high, the cells may detach from the chamber slide.
8. The receptor binding affinity of fluorescent probe can also be determined by cell-based receptor-binding assay.
9. Animals are fed with alfalfa-free diet, such as 2018 Teklad global 18% protein rodent diet (Harlan Laboratories, Livermore, CA, USA) for 2 weeks prior to tumor implantation and maintained on the same diet throughout the study to minimize autofluorescence and improve imaging clarity.
10. Based on the pharmacokinetics of fluorescent probe, the imaging time points can be varied.
11. To investigate the biodistribution of fluorescent probe, ex vivo NIRF imaging can be performed. After injection of fluorescent probe at a certain time point, tumors, tissues, and organs are dissected and subjected to ex vivo NIRF imaging. The uptake of fluorescent probe can be quantified by the ROI analysis of images.
12. Statistical analysis is performed with a Student's *t* test. Statistical significance is assigned for P values < 0.05.

Acknowledgments

This work was supported by the American Cancer Society (#IRG-58-007-51), the Robert E. and May R. Wright Foundation, and the USC Department of Radiology.

References

1. Weissleder R, Tung CH, Mahmood U, Bogdanov A Jr (1999) In vivo imaging of tumors with protease-activated near-infrared fluorescent probes. Nat Biotechnol 17(4):375–378
2. Tung CH (2004) Fluorescent peptide probes for in vivo diagnostic imaging. Biopolymers 76(5):391–403
3. Chen X, Conti PS, Moats RA (2004) In vivo near-infrared fluorescence imaging of integrin alphavbeta3 in brain tumor xenografts. Cancer Res 64(21):8009–8014
4. Kobayashi H, Ogawa M, Alford R, Choyke PL, Urano Y (2010) New strategies for fluorescent probe design in medical diagnostic imaging. Chem Rev 110(5):2620–2640
5. Chen K, Yap LP, Park R, Hui X, Wu K, Fan D, Chen X, Conti PS (2012) A Cy5.5-labeled phage-displayed peptide probe for near-infrared

fluorescence imaging of tumor vasculature in living mice. Amino Acids 42(4):1329–1337

6. Li G, Xing Y, Wang J, Conti PS, Chen K (2014) Near-infrared fluorescence imaging of CD13 receptor expression using a novel Cy5.5-labeled dimeric NGR peptide. Amino Acids 46(6):1547–1556
7. Raymond SB, Skoch J, Hills ID, Nesterov EE, Swager TM, Bacskai BJ (2008) Smart optical probes for near-infrared fluorescence imaging of Alzheimer's disease pathology. Eur J Nucl Med Mol Imaging 35(Suppl 1):S93–S98
8. Wunderbaldinger P, Turetschek K, Bremer C (2003) Near-infrared fluorescence imaging of lymph nodes using a new enzyme sensing activatable macromolecular optical probe. Eur Radiol 13(9):2206–2211
9. Sakatani K, Kashiwasake-Jibu M, Taka Y, Wang S, Zuo H, Yamamoto K, Shimizu K (1997) Noninvasive optical imaging of the subarachnoid space and cerebrospinal fluid pathways based on near-infrared fluorescence. J Neurosurg 87(5):738–745
10. Chen K, Chen X (2011) Positron emission tomography imaging of cancer biology: current status and future prospects. Semin Oncol 38(1):70–86
11. Chen K, Conti PS (2010) Target-specific delivery of peptide-based probes for PET imaging. Adv Drug Deliv Rev 62(11):1005–1022
12. Cai W, Gambhir SS, Chen X (2008) Chapter 7. Molecular imaging of tumor vasculature. Methods Enzymol 445:141–176
13. Huang R, Wang M, Zhu Y, Conti PS, Chen K (2015) Development of PET probes for cancer imaging. Curr Top Med Chem 15(8):795–819
14. Ellis LM, Liu W, Ahmad SA, Fan F, Jung YD, Shaheen RM, Reinmuth N (2001) Overview of angiogenesis: biologic implications for antiangiogenic therapy. Semin Oncol 28(5 Suppl 16):94–104
15. Kuwano M, Fukushi J, Okamoto M, Nishie A, Goto H, Ishibashi T, Ono M (2001) Angiogenesis factors. Intern Med 40(7):565–572
16. Yancopoulos GD, Davis S, Gale NW, Rudge JS, Wiegand SJ, Holash J (2000) Vascular-specific growth factors and blood vessel formation. Nature 407(6801):242–248
17. Bhagwat SV, Lahdenranta J, Giordano R, Arap W, Pasqualini R, Shapiro LH (2001) CD13/APN is activated by angiogenic signals and is essential for capillary tube formation. Blood 97(3):652–659
18. Guzman-Rojas L, Rangel R, Salameh A, Edwards JK, Dondossola E, Kim YG, Saghatelian A, Giordano RJ, Kolonin MG, Staquicini FI, Koivunen E, Sidman RL, Arap W, Pasqualini R (2012) Cooperative effects of aminopeptidase N (CD13) expressed by nonmalignant and cancer cells within the tumor microenvironment. Proc Natl Acad Sci U S A 109(5):1637–1642
19. Teranishi J, Ishiguro H, Hoshino K, Noguchi K, Kubota Y, Uemura H (2008) Evaluation of role of angiotensin III and aminopeptidases in prostate cancer cells. Prostate 68(15):1666–1673
20. Ikeda N, Nakajima Y, Tokuhara T, Hattori N, Sho M, Kanehiro H, Miyake M (2003) Clinical significance of aminopeptidase N/CD13 expression in human pancreatic carcinoma. Clin Cancer Res 9(4):1503–1508
21. Hashida H, Takabayashi A, Kanai M, Adachi M, Kondo K, Kohno N, Yamaoka Y, Miyake M (2002) Aminopeptidase N is involved in cell motility and angiogenesis: its clinical significance in human colon cancer. Gastroenterology 122(2):376–386
22. Arap W, Pasqualini R, Ruoslahti E (1998) Cancer treatment by targeted drug delivery to tumor vasculature in a mouse model. Science 279(5349):377–380
23. Pasqualini R, Koivunen E, Kain R, Lahdenranta J, Sakamoto M, Stryhn A, Ashmun RA, Shapiro LH, Arap W, Ruoslahti E (2000) Aminopeptidase N is a receptor for tumor-homing peptides and a target for inhibiting angiogenesis. Cancer Res 60(3):722–727
24. von Wallbrunn A, Waldeck J, Holtke C, Zuhlsdorf M, Mesters R, Heindel W, Schafers M, Bremer C (2008) In vivo optical imaging of CD13/APN-expression in tumor xenografts. J Biomed Opt 13(1):011007
25. Negussie AH, Miller JL, Reddy G, Drake SK, Wood BJ, Dreher MR (2010) Synthesis and in vitro evaluation of cyclic NGR peptide targeted thermally sensitive liposome. J Control Release 143(2):265–273
26. Wang RE, Niu Y, Wu H, Amin MN, Cai J (2011) Development of NGR peptide-based agents for tumor imaging. Am J Nucl Med Mol Imaging 1(1):36–46
27. Shao Y, Liang W, Kang F, Yang W, Ma X, Li G, Zong S, Chen K, Wang J (2014) 68Ga-labeled cyclic NGR peptide for MicroPET imaging of CD13 receptor expression. Molecules 19(8): 11600–11612
28. Li G, Wang X, Zong S, Wang J, Conti PS, Chen K (2014) MicroPET imaging of CD13 expression using a ^{64}Cu-labeled dimeric NGR peptide based on sarcophagine cage. Mol Pharm 11(11):3938–3946
29. Ma W, Kang F, Wang Z, Yang W, Li G, Ma X, Li G, Chen K, Zhang Y, Wang J (2013) ^{99m}Tc-labeled monomeric and dimeric NGR peptides for SPECT imaging of CD13 receptor in tumor-bearing mice. Amino Acids 44(5):1337–1345
30. Chen K, Ma W, Li G, Wang J, Yang W, Yap LP, Hughes LD, Park R, Conti PS (2013) Synthesis

and evaluation of ^{64}Cu-labeled monomeric and dimeric NGR peptides for microPET imaging of CD13 receptor expression. Mol Pharm 10(1):417–427

31. Kolb HC, Sharpless KB (2003) The growing impact of click chemistry on drug discovery. Drug Discov Today 8(24):1128–1137
32. Nwe K, Brechbiel MW (2009) Growing applications of "click chemistry" for bioconjugation in contemporary biomedical research. Cancer Biother Radiopharm 24(3):289–302
33. Chen K, Wang X, Lin W, Shen K-F, Yap LP, Hughes LD, Conti PS (2012) Strain-promoted catalyst-free click chemistry for rapid construction of ^{64}Cu-labeled PET imaging probes. ACS Med Chem Lett 3(12):1019–1023
34. Debets MF, van Berkel SS, Schoffelen S, Rutjes FP, van Hest JC, van Delft FL (2010) Aza-dibenzocyclooctynes for fast and efficient enzyme PEGylation via copper-free (3+2) cycloaddition. Chem Commun 46(1):97–99
35. Debets MF, van Berkel SS, Dommerholt J, Dirks AT, Rutjes FP, van Delft FL (2011) Bioconjugation with strained alkenes and alkynes. Acc Chem Res 44(9):805–815
36. Luo S, Zhang E, Su Y, Cheng T, Shi C (2011) A review of NIR dyes in cancer targeting and imaging. Biomaterials 32(29):7127–7138